Global Advanced Research Journal of Engineering, Technology and Innovation (ISSN: 2315-5124) Vol. 2(5) pp. 144-152, June, 2013
Available online http://garj.org/garjeti/index.htm

Full Length Research Paper

Task-space control of flexible-joint electrically driven robots

Mohammad Mehdi Fateh and Alireza Izadbakhsh*

Department of Electrical Engineering, Shahrood University of Technology, Shahrood, Iran

Accepted 02 June 2013

This paper presents a novel robust decentralized controller for flexible-joint electrically driven robots under the imperfect transformation of control space, from Task-Space (TS) to Joint-Space (JS). The proposed approach is free from manipulator dynamics, thus free from problems associated with torque control strategy in the design and implementation. As a result, the proposed control is simple, fast response and superior to torque control approaches. It can guarantee robustness of control system to both structured and unstructured uncertainties associated with robot dynamics. The control method is verified by stability analysis. Simulations on a two-link actuated flexible-joint robot show the effectiveness of the proposed control approach.

Keywords: Robust control, voltage control strategy, flexible-joint electrically driven robots.

INTRODUCTION

Motion control of robot manipulators has been studied using various approaches, such as PD control (Tomei, 1991), feedback linearization (Luca et al., 1985), integral manifold approach (Spong et al., 1987), singular perturbation theory (Subudhi and Morris, 2006), robust control (Spong, 1987), sliding mode control (Spurgeon et al., 2001), fuzzy control (Chen, 2011), adaptive control (Ghorbel et al., 1989), back stepping control (Lee et al., 2007), state observer based control (Talole et al., 2010), neural network approach (Zeman et al., 1997), and learning control (Wang, 1995) under uncertainties. A major problem, common in all aforementioned control strategies is performing the control law in the JS, while the goal of many robotic control tasks are generally to move the tool center point of the arm along a given trajectory in the TS. Thus, despite of well behavior of aforementioned control strategies in joint space, none of them can provide satisfactory tracking performances in TS under the imperfect transformation of control space from Cartesian to joint angles. Some of these reasons are as follow :

- The robot’s kinematics and dynamics change when a manipulator picks up different tools of unknown length, or unknown gripping points (Cheah et al., 2010). Therefore, the desired joint angles, their velocities, and accelerations are not produced precisely in JS under the imperfect transformation from TS to JS.
- Tracking errors are appeared in TS while actuators operate in JS. Thus, transforming of control space should be carried out to perform a control law (Fateh and Farhangfard, 2008). As a fast result, the control inputs involve errors if we use the imperfect transformation
- The produced tracking errors in workspace are not detectable and compensable appropriately due to lack of feedbacks from the end-effector.

To deal with this problem, feedbacks from TS are required to detect tracking error in TS Colbaugh and

*Corresponding Author’s Email: izadbakhsh_alireza@hotmail.com

Glass, 1997; Hu and Vukovich, 2001; Tian et al., 2004; Tian and Goldenberg, 1995; Faroog et al., 2008; Goldsmith et al., 1999). Based on this observation, the TS controllers were then developed using assumption of perfect transformation in control spaces. However, there is yet problems arises from dynamic formulation of robot manipulators in TS, that involves strong couplings between the joint motions, the time derivative of jacobian matrix, as well as its inverse transformation. Recently, a number of approximate Jacobian controllers have been presented to cope with the uncertain robot kinematics and dynamics by using adaptive control laws. The proposed controller does not require the exact knowledge of the kinematics and Jacobian matrix (Liu et al., 2008). However, they are unable to handle unstructured uncertainties in the control space transformation. To solve this problem (Chien and Huang, 2010), presented a valuable work, although it has required to considerable burden of computer computations.

So far, robot manipulators have been frequently controlled using the torque-control strategy. It must be noted that, although torque controllers are frequently used for controlling robotic manipulators, the role of actuator dynamics considered by voltage control in some cases cannot be neglected. Indeed, torque controllers have some limitations coming from practical point of view as follows:

- A torque control law cannot be given directly to the torque inputs of an electrical manipulator. Because, physical control variables are electrical signals to the actuators not the torque vector applied to the robot joints.
- The dynamics of motors and drives are excluded in the torque control strategies, while the actuator dynamics are often a source of uncertainty due to e.g. calibration errors, or parameter variation from overheating and changes in environment temperature (Cheah et al., 2010).
- The control problem becomes hypersensitive when tracking the fast trajectories are demanded. Therefore, control performance degrades quickly as speed increases.
- Some torque control approaches try to cancel the nonlinearities by using feedbacks from the joint torques. However, they face some challenging problems (Morris, 2001).

Three customary approaches in this category:

- using reaction force in the shaft bearings
- Prony brake method
- using strain gages in rotating body

suffer from several inherent weaknesses. The first method is involved bearing friction and windage torques which are not avoidable. The second approach requires some additional devices which are not convenient. Finally, the third method is expensive with difficulty of installation. To overcome these drawbacks, voltage control strategy was proposed (Fateh, 2008). This strategy is free from manipulator dynamics in a decentralized structure. All nonlinearities associated with robot dynamics are canceled by feedback linearization through feedbacks from motor currents. Following this strategy, the adaptive control (Fateh, 2012) and robust control (Fateh, 2012) were developed for flexible-joint robots. The proposed approaches are superior to torque controller in terms of simplicity of design, ease of implementation and control performance. However, the TS implementations of these type controllers remain as an open question for electrically driven flexible joint robots. Due to the aforementioned problems, we are interested in developing a novel robust control approach under the imperfect transformation of control space. The proposed controller includes two interior loops. The inner loop controls the motor position using SMC technique, while the outer loop control generates a desired motor position for inner loop via controlling the joint angle by a simple PID controller. The contributions of this paper are as follows. Nonlinear dynamic description is studied in Section 2. The overall control structure of the robust JS control design will be outlined in Section 3 and the closed-loop system stability is then presented in Section 4. An extension of the proposed JS control strategy is presented in section 5. In Section 6 the validity of the proposed method is verified by computer simulation. Finally, we give our conclusion remarks in Section 7.

Dynamics of electrically driven flexible joint robot

In the flexible joint robot arm, the link dynamics are actuated by the spring torque produced by the difference between the motor displacements on the link side elements of transmission mechanism, and link angular positions. The motor dynamics are also driven by the motor torque. Thus, the robot dynamics with joint flexibility can be described as [25]

$$\boldsymbol{D}(\boldsymbol{q})\ddot{\boldsymbol{q}}+\boldsymbol{C}(\boldsymbol{q},\dot{\boldsymbol{q}})\dot{\boldsymbol{q}}+\boldsymbol{g}(\boldsymbol{q})=\boldsymbol{K}(\boldsymbol{r}\boldsymbol{\theta}-\boldsymbol{q}) \quad (1)$$

$$\boldsymbol{J_m}\ddot{\boldsymbol{\theta}}+\boldsymbol{B_m}\dot{\boldsymbol{\theta}}+\boldsymbol{r}\boldsymbol{K}(\boldsymbol{r}\boldsymbol{\theta}-\boldsymbol{q})=\boldsymbol{\tau} \quad (2)$$

where $\boldsymbol{\theta}\in\mathbb{R}^{n\times1}$ and $\boldsymbol{q}\in\mathbb{R}^{n\times1}$ represent respectively the vectors of link positions and motor angular positions, $\boldsymbol{K}\in\mathbb{R}^{n\times n}$ is a diagonal positive definite matrix representing the joint stiffness, $\boldsymbol{D}(\boldsymbol{q})\in\mathbb{R}^{n\times n}$ is the symmetric positive definite manipulator inertia matrix, $\boldsymbol{C}(\boldsymbol{q},\dot{\boldsymbol{q}})\dot{\boldsymbol{q}}\in\mathbb{R}^{n\times1}$ is a vector function containing Coriolis and centrifugal forces, $\boldsymbol{g}(\boldsymbol{q})\in\mathbb{R}^{n\times1}$ is a vector function containing of gravitational forces, $\boldsymbol{r}$ is an $n\times n$ transmission matrix, $\boldsymbol{J_m}\in\mathbb{R}^{n\times n}$ is a diagonal matrix of the lumped actuator rotor inertias, $\boldsymbol{B_m}\in\mathbb{R}^{n\times n}$ is diagonal matrix of the lumped actuator damping coefficients, and $\boldsymbol{\tau} \in \mathbb{R}^{n\times1}$ is the vector of actuator input torque produced by

$$\boldsymbol{\tau} = \boldsymbol{k_m I} \qquad (3)$$

where $\boldsymbol{k_m} \in \mathbb{R}^{n\times n}$ is a positive definite constant diagonal matrix characterizing the electro-mechanical conversion between armature current $\boldsymbol{I} \in \mathbb{R}^{n\times1}$ and the motor torque. Now, due to have motor voltages as the inputs for electrical flexible-joint robot, some modifications are required. Toward this end, consider the electrical equation of permanent magnet DC motors in the matrix from as

$$\boldsymbol{L\dot{I}} + \boldsymbol{RI} + \boldsymbol{k_b\dot{\theta}} + \boldsymbol{\phi}(t) = \boldsymbol{u} \qquad (4)$$

where $\boldsymbol{L} \in \mathbb{R}^{n\times n}$ is a constant diagonal matrix of electrical inductance, $\boldsymbol{R} \in \mathbb{R}^{n\times n}$ is diagonal matrix of armature resistances, $\boldsymbol{k_b} \in \mathbb{R}^{n\times n}$ is a diagonal constant matrix for the back-emf effects, $\boldsymbol{u} \in \mathbb{R}^{n}$ is the control input voltage applied for the joint actuators, and $\boldsymbol{\phi}(t)$ represents an external disturbance. Let us using the state variables $\boldsymbol{x}_1 = \boldsymbol{q}$, $\boldsymbol{x}_2 = \dot{\boldsymbol{q}}$, $\boldsymbol{x}_3 = \boldsymbol{\theta}$, $\boldsymbol{x}_4 = \dot{\boldsymbol{\theta}}$, and $\boldsymbol{x}_5 = \boldsymbol{I}$ in the state vector

$$\mathbf{x}^{\boldsymbol{T}} = \begin{bmatrix} \boldsymbol{q} & \dot{\boldsymbol{q}} & \boldsymbol{\theta} & \dot{\boldsymbol{\theta}} & \boldsymbol{I} \end{bmatrix} \qquad (5)$$

Then, the state space model using equations (1)-(4) is represented as:

$$\dot{\mathbf{x}} = \boldsymbol{f}(\mathbf{x}) + \mathbf{B}\boldsymbol{u} - \mathbf{B}\boldsymbol{\phi}(t) \qquad (6)$$

with

$$\boldsymbol{f}(\mathbf{x}) = \begin{bmatrix} \boldsymbol{x}_2 \\ \boldsymbol{D}^{-1}(\boldsymbol{x}_1)\left(-\boldsymbol{C}(\boldsymbol{x}_1,\boldsymbol{x}_2)\boldsymbol{x}_2 - \boldsymbol{g}(\boldsymbol{x}_1) + \boldsymbol{K}(\boldsymbol{r}\boldsymbol{x}_3 - \boldsymbol{x}_1)\right) \\ \boldsymbol{x}_4 \\ \boldsymbol{J_m}^{-1}\left(-\boldsymbol{B_m}\boldsymbol{x}_4 + \boldsymbol{rK}(\boldsymbol{x}_1 - \boldsymbol{r}\boldsymbol{x}_3) + \boldsymbol{k_m}\boldsymbol{x}_5\right) \\ -\boldsymbol{L}^{-1}\left(\boldsymbol{R}\boldsymbol{x}_5 + \boldsymbol{k_b}\boldsymbol{x}_4\right) \end{bmatrix}$$

$$\mathbf{B} = \begin{bmatrix} 0 & 0 & 0 & 0 & \boldsymbol{L}^{-1} \end{bmatrix}^{\boldsymbol{T}} \qquad (7)$$

As can be seen from (6), and (7), the presented model includes serious problems such as, nonlinearities, uncertainties, flexibility in the joint, as well as couplings between the joint motions. To control such a complicated system, we propose a *decentralized* robust control scheme using voltage control strategy. The general idea behind the notion of voltage control strategy is that, the motor current contains the effects of all uncertainties and coupling between the motor and the manipulator. Thus, canceling this coupling will obtain a control law that is free from manipulator dynamics.

Robust JS control design

In this section, we are interested in deriving a control law such that in the closed-loop system, the link angles track the desired trajectory with an acceptable error. For this purpose, we propose a controller that includes two interior loops. The inner loop controls the motor position using SMC technique, while the outer loop generates a desired motor position θ_d for inner loop by a simple PID controller.

Inner loop control design

Suppose that equation (4) can be rewritten based on the nominal model parameters as

$$\hat{R}I + \hat{k}_b\dot{\theta} + \eta(t) = u \qquad (8)$$

where $(\hat{\cdot})$ denotes an estimation of $(\cdot)$, and

$$\eta(t) = L\dot{I} + (R - \hat{R})I + (k_b - \hat{k}_b)\dot{\theta} + \phi(t) \qquad (9)$$

represent the disturbances caused by the unmodeled dynamics, model uncertainties, and external disturbances. Let us define a switching surface as

$$S_\theta = e(t) + c_1\int_0^t e(\tau)d\tau \quad , \quad t \geq 0 \qquad (10)$$

where $e(t) = \theta_d - \theta$, and c_1 denotes a positive diagonal matrix. This choice of sliding surface is preferred since it is linear and it will result in a relative degree one dynamic. Now, it must be founded a control input u such that, the state trajectory converges to the switching surface. In the following, we will employ the direct lyapunov method to derivate a sliding mode control law that guarantees the stability of sliding surface. Differentiating S_θ with respect to time obtains

$$\dot{S}_\theta = \dot{\theta}_d - \hat{k}_b^{-1}u + \hat{k}_b^{-1}\hat{R}I + \hat{k}_b^{-1}\eta(t) + c_1e(t) \qquad (11)$$

Thus, the actuator voltage controller can be designed as

$$u = \hat{R}I + \hat{k}_b\dot{\theta}_d + \hat{k}_bc_1e(t) + \rho sign\left(S_\theta\right) \qquad (12)$$

where ρ is a positive real constant which is determined based on bounding function on the uncertainties. We refer to (12) as the inner loop control law. The term θ_d in (12), which we refer to it as the outer loop control, represents a new input which is designed in section 3.2.

Proof: Choose a non negative function

$$V = \frac{1}{2}S_\theta^2 \geq 0 \qquad (13)$$

Differentiating V respect to time, and using (11) and (12) obtains

$$\begin{aligned} \dot{V} &= S_\theta\dot{S}_\theta = S_\theta\hat{k}_b^{-1}\left(\eta(t) - \rho sign\left(S_\theta\right)\right) \\ &\leq \left|S_\theta\right|\hat{k}_b^{-1}\left(\left|\eta(t)\right| - \rho\right) \end{aligned} \qquad (14)$$

Now, the sufficient condition to establish $\dot{V} < 0$ is

$$\left|\eta(t)\right| < \rho \qquad (15)$$

Therefore, with the controller (12), the sliding surface brcomes attractive. It must be emphasized that, by choosing control law in the form (12), chattering phenomena will occur because of discontinuity in signum function. To reduce this effect, a continuous approximation of the switching controller is used instead of the signum function. Hence, the alternative control signal in (12) becomes:

$$u = \hat{R}I + \hat{k}_b\dot{\theta}_d + \hat{k}_b c_1 e(t) + \rho sat\left(\frac{S_\theta}{\varepsilon}\right) \quad (16)$$

where

$$sat(\square) = \begin{cases} sign(\square) & |\square| \geq 1 \\ (\square) & |\square| < 1 \end{cases} \quad (17)$$

and ε is a positive constant, called the boundary layer of the sliding surface. This completes stability proof for inner loop control design.

Outer loop control design

Here, the control objective is, to design a desired trajectory θ_d for the inner loop controller, so that $\theta \to \theta_d$ which further implies convergence of the q to the desired trajectory q_d. Based on this observation, we propose

$$\theta_d = K_d\dot{E}(t) + K_p E(t) + K_i\int_0^t E(\tau)d\tau \quad , \quad t \geq 0 \quad (18)$$

where K_d, K_p, K_i are diagonal matrices with positive diagonal elements and

$$E(t) = q_d - q \quad (19)$$

is the JS tracking error. Since, the voltage of every motor should be limited to protect the motor against over voltages, therefore by using a voltage limiter, we obtain

$$u(t) = v \quad , \quad \text{for } |v| \leq v_{\max} \quad (20)$$

$$u(t) = v_{\max}\text{sign(v)} \quad , \quad \text{for } |v| > v_{\max} \quad (21)$$

where $v_{\max}$ is positive constant called as the maximum permitted voltage of motor and v is expressed as

$$v = \hat{R}I + \hat{k}_b\dot{\theta}_d + \hat{k}_b c_1 e(t) + \rho sat\left(\frac{S_\theta}{\varepsilon}\right) \quad (22)$$

ANALYSIS

Due to decentralized characteristic of the proposed controller, stability analysis is presented separately for every individual joint to verify stability of the robotic system.

The control law (20)-(22) implies that the motor voltage is limited. Thus, we can assume that:

Assumption 1: $|u(t)| \leq v_{\max}$ (23)

To make the dynamics of the tracking error well defined such that the robot can track the desired trajectory, we make the following assumption.

Assumption 2: The JS desired trajectory q_d, the TS desired trajectory X_d and their derivatives up to a necessary order are available and all uniformly bounded. A robust controller can be designed if the external disturbance be bounded. Thus

Assumption 3: The external disturbance $\phi(t)$ is bounded as

$$\|\phi(t)\| \leq \phi_{\max} \quad (24)$$

where $\phi_{\max}$ is a positive constant.

Since, the control laws given by (20)-(22), operate in two areas, i.e, $|v| \leq v_{\max}$ and $|v| > v_{\max}$, thus, tracking performance should be evaluated in both areas.

Area of $|v| \leq v_{\max}$

In this area, we have

$$u(t) = \hat{R}I + \hat{k}_b\dot{\theta}_d + \hat{k}_b c_1 e(t) + \rho sat\left(\frac{S_\theta}{\varepsilon}\right) \quad (25)$$

Substituting (25) into (8), rearranging with some mathematical simplification yields the dynamics of the motor position tracking loop as

$$\dot{e}(t) + c_1 e(t) = \left(\hat{k}_b^{-1}\right)\left(\eta(t) - \rho sat\left(\frac{S_\theta}{\varepsilon}\right)\right) \quad (26)$$

The variables $\dot{\theta}$, I, and $\dot{I}$ are bounded since u is bounded [25]. These results, in addition to assumption 3, obtains the function bounding the uncertainty on the RHS of equation (26) as

$$\left|\eta(t) - \rho sat\left(\frac{S_\theta}{\varepsilon}\right)\right| \leq L\dot{I}_{\max} + \zeta_1 I_{\max} + \zeta_2\dot{\theta}_{\max} + \phi_{\max} + \rho = \psi \quad (27)$$

where $(\bullet)_{\max}$ is a positive scalar function, representing the upper bound of $(\bullet)$, and ζ_1 and ζ_2 are positive constants and the upper bounds of $(R - \hat{R})$ and $(k_b - \hat{k}_b)$, respectively. Thus, $e(t)$ and $\dot{e}(t)$ are bounded, that means boundedness of $\dot{\theta}_d = \dot{\theta} - \dot{e}(t)$ since $\dot{\theta}$ and $\dot{e}(t)$ are bounded. Differentiating (18) with respect o time, yields

$$K_d\ddot{E}(t) + K_p\dot{E}(t) + K_i E(t) = \dot{\theta}_d \quad (28)$$

which is a 2nd order LTI system with positive gains K_d, K_p and K_i with limited input $\dot{\theta}_d$. This system is stable based on the Routh-Hurwitz criterion. Thus $E(t)$, $\dot{E}(t)$ and $\ddot{E}(t)$ are bounded. From assumption 2 q_d, $\dot{q}_d$ and $\ddot{q}_d$ and consequently q, $\dot{q}$ and $\ddot{q}$ are also bounded. Finally, from (2) and (3), we have

$$J_m\ddot{\theta}+B_m\dot{\theta}+r^2K\theta=k_mI+rKq \quad (29)$$

which represent a stable 2nd order LTI system driven by the bounded input k_mI+rKq. Thus, θ, $\dot{\theta}$, and $\ddot{\theta}$ are bounded. Since, all states θ, $\dot{\theta}$, q, $\dot{q}$, and I associated with each joint are bounded then vectors $\boldsymbol{\theta}$, $\dot{\boldsymbol{\theta}}$, $\boldsymbol{q}$, $\dot{\boldsymbol{q}}$, and $\boldsymbol{I}$ are bounded. As a result, the robotic system has the Bounded Input-Bounded Output (BIBO) stability.

Area of $|v|>v_{\max}$

In this area, we have

$$L\dot{I}+RI+k_b\dot{\theta}+\phi(t)=v_{\max}\text{sign}(v) \quad (30)$$

To consider the convergence of tracking error $e(t)$ in this area, a positive definite function is proposed as

$$V=\frac{1}{2}k_be^2(t)\geq 0 \quad (31)$$

By differentiating V respect to time, using $e(t)=\theta_d-\theta$ and (30), we have

$$\dot{V}=e(t)\left(k_b\dot{\theta}_d+L\dot{I}+RI+\phi(t)-v_{\max}\text{sign}(v)\right) \quad (32)$$

Assume that, there exists a positive scalar denoted by μ that

$$\left|L\dot{I}+RI+k_b\dot{\theta}_d+\phi(t)\right|<\mu \quad (33)$$

Thus, to establish the convergence, $\dot{V}<0$, it is sufficient that

$$v_{\max}\text{sign}(v)=\mu\text{sign}(e) \quad (34)$$

Proof: Substituting (34) into (32) yields

$$\dot{V}=e(t)\left(k_b\dot{\theta}_d+L\dot{I}+RI+\phi(t)-\mu\text{sign}(e)\right) \quad (35)$$

Now, for $\dot{V}$ to be a negative definite function, the requirement is (33)

$$\begin{aligned}\dot{V}&\leq|e(t)|\left|k_b\dot{\theta}_d+L\dot{I}+RI+\phi(t)\right|-\mu e(t)\text{sign}\left(e(t)\right)\\&=|e(t)|\left|L\dot{I}+RI+\phi(t)+k_b\dot{\theta}_d\right|-\mu|e(t)| \quad (36)\\&=|e(t)|\left(\left|L\dot{I}+RI+\phi(t)+k_b\dot{\theta}_d\right|-\mu\right)\end{aligned}$$

Thus, taking (33) into account, it implies that, the motor tracking error is converged until the control system comes into the area governed by control law (20). As a result, even if the robotic system starts from the area of $|v|>v_{\max}$, it goes into the area of $|v|\leq v_{\max}$, that all states are bounded. Equation (34) means that

$$v_{\max}=\mu \quad (37)$$

Therefore, the maximum voltage of motor should satisfy (37) for the convergence of position tracking error $e(t)$. From the closed loop system (30), we can obtain

$$L\dot{I}+RI=v_{\max}\text{sign}(v)-k_b\dot{\theta}-\phi(t) \quad (38)$$

which is a stable first order LTI system driven by the bounded input $v_{\max}\text{sign}(v)-k_b\dot{\theta}-\phi(t)$. Thus, I is bounded. Since I is limited, then, linear stable system (29) under bounded input k_mI+rKq obtains that variables θ, $\dot{\theta}$, and $\ddot{\theta}$ are bounded. Consider (28) as a second order linear system with positive gains K_d, K_p, K_i, and a limited input $\dot{\theta}_d$. Thus E, $\dot{E}$, and $\ddot{E}$ are bounded. According to assumption 2, q_d and its time derivatives are bounded that result in boundedness of q, $\dot{q}$, and $\ddot{q}$. Thus, the robotic system has the Bounded Input-Bounded Output (BIBO) stability. This is because the system states, i.e., $\boldsymbol{\theta}$, $\dot{\boldsymbol{\theta}}$, $\boldsymbol{q}$, $\dot{\boldsymbol{q}}$, and $\boldsymbol{I}$ are bounded.

Robust TS control design

As mentioned before, in the most of robotic applications, a desired path is specified for the end-effector in the TS, while the actuators operate in the JS. Thus, transformation of control space is unavoidable. It is clear that, despite of well behavior of JS control strategies, none of them can provide satisfactory tracking performances in TS under the imperfect transformation of control space.

Toward this end, here, we will improve the outer-loop of the proposed JS controller to track a desired path in TS. Let us $X\in\mathbb{R}^n$ to be a TS vector, representing the position and orientation of the robot end-effecor relative to a fixed user defined reference frame.

Then, the forward kinematic and differential kinematic transformation between the robot links coordinates and the end-effector coordinates can be written as

$$X=h(q) \quad (39)$$

$$\dot{X}=J(q)\dot{q} \quad (40)$$

where $h(q):\mathbb{R}^n\rightarrow\mathbb{R}^n$ is the differentiable forward kinematics of the manipulator, and $J(q)\in\mathbb{R}^{n\times n}$ denotes the Jacobian matrix defined as $J(q)=\partial h(q)/\partial q\in\mathbb{R}^{n\times n}$. Now, we propose the outer-loop controller in the form

$$\theta_d=\int_0^t\hat{J}^{-1}(q)(K_d\ddot{E}_x(\tau)+K_p\dot{E}_x(\tau)+K_iE_x(\tau))d\tau \quad ,\ t\geq 0 \quad (41)$$

where

$$E_x=X_d-X \quad (42)$$

denotes the TS position error and X_d is the desired position vector. The block diagram of the proposed control approach is shown in Figure. 1. By the similar stability analysis, as the same as previous section, we will evaluate the closed-loop system performance in both areas.

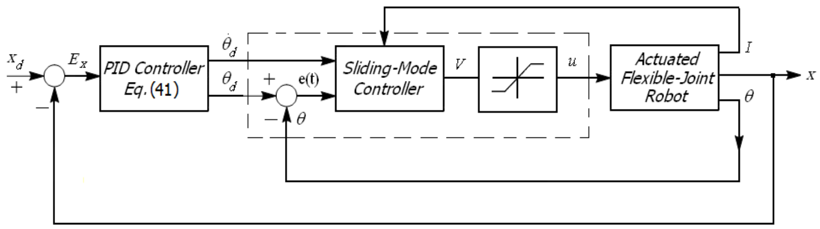

Figure.1. Inner-loop controller (dashed box) with the outer-loop controller

Area of $|v| \leq v_{max}$

As shown in previous section, the RHS of (26), $e(t)$ and therefore $\dot{e}(t)$ are bounded. Thus, boundedness of $\dot{\theta}_d = \dot{\theta} - \dot{e}(t)$ can be achieved, whereas, $\dot{\theta}$, and $\dot{e}(t)$ are bounded. Differentiating both side of (41) with respect to time gives

$$K_d \ddot{E}_x + K_p \dot{E}_x + K_i E_x = \hat{J}\dot{\theta}_d \qquad (43)$$

which is a second order linear system with positive gains and a limited input $\hat{J}\dot{\theta}_d$, since $\hat{J}$ is a combination of sine and cosine functions. Thus, E_x, $\dot{E}_x$, $\ddot{E}_x$ and therefore X, $\dot{X}$, and $\ddot{X}$ are bounded from assumption 2. As a conclusion of this analysis, the robotic system has the BIBO stability in this area, since all of system states are bounded.

Area of $|v| > v_{\max}$

Choosing a positive definite function as the same as (31) shows that, the value of $|e(t)|$ reduces by starting from any arbitrary initial value of $e(0)$ under the condition (37). Thus, motor will move to to the area of $|v| \leq v_{\max}$ that all signals are bounded. As a result, boundedness of I, θ, $\dot{\theta}$, and $\ddot{\theta}$ can be achieved as same as section 4.2. Consider (43) as a second order linear system with positive gains K_d, K_p, K_i and a limited input $\hat{J}\dot{\theta}_d$. Thus, E_x, $\dot{E}_x$, and $\ddot{E}_x$ are bounded. From $E_x = X_d - X$, $\dot{E}_x = \dot{X}_d - \dot{X}$, $\ddot{E}_x = \ddot{X}_d - \ddot{X}$, and using assumption 2, it follows that X, $\dot{X}$, and therefore $\ddot{X}$ are bounded. This completes the proof. As a conclusion of this analysis, the robotic system has the BIBO stability.

Computer simulation

The robust performance of the proposed control strategy was verified through simulations of a two-link electrically driven robot manipulator with flexible joints, uncertainty in the motor dynamics and without any knowledge of the manipulator dynamic. The dynamic model of the robot system can be described in the form of (1):

$$D(q) = \begin{bmatrix} d_{11} & d_{12} \\ d_{21} & d_{22} \end{bmatrix}$$

$$d_{11} = m_2\left(l_1^2 + l_{c2}^2 + 2l_1 l_{c2} cos(q_2)\right) + m_1 l_{c1}^2 + I_1 + I_2$$

$$d_{21} = d_{12} = m_2 l_{c2}^2 + m_2 l_1 l_{c2} cos(q_2) + I2$$

$$d_{22} = m_2 l_{c2}^2 + I_2$$

$$C(q,\dot{q})\dot{q} = \begin{bmatrix} -2m_2 l_1 l_{c2} sin(q_2)\left(\dot{q}_1\dot{q}_2 + 0.5\dot{q}_2^2\right) \\ m_2 l_1 l_{c2} sin(q_2)\dot{q}_1^2 \end{bmatrix}$$

$$g(q) = \begin{bmatrix} (m_1 l_{c1} + m_2 l_1)\, g cos(q_1) + m_2 l_{c2} g cos(q_1 + q_2) \\ m_2 l_{c2} g cos(q_1 + q_2) \end{bmatrix} \qquad (44)$$

where q_1 and q_2 are the angle of joints 1 and 2, m_1 and m_2 are the mass of links 1 and 2 respectively, l_1 and l_2 are the length of links 1 and 2, I_i is the link's moment of inertia given in center of mass, l_{ci} is the distance between the center of mass of link and the i*th* joint, and g is the gravity acceleration. The manipulator dynamic parameters are defined as $l_1 = l_2 = 1m$, $l_{c1} = l_{c2} = 0.5m$, $m_1 = 15kg$ and $m_2 = 6kg$, $I_1 = 5\ kg\text{-}m^2$ and $I_2 = 2\ kg\text{-}m^2$; Also, the exact-actuator dynamic model parameters are selected as

.

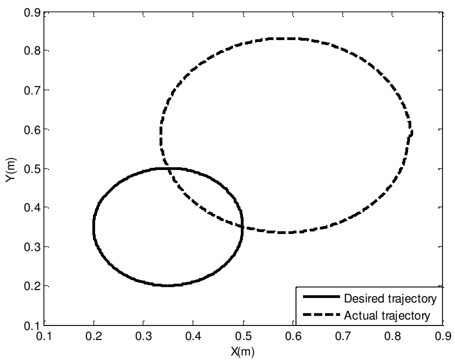

Figure 2 Tracking performance in TS

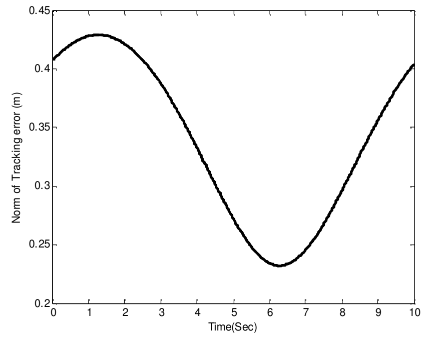

Figure 3 Norm of tracking error in TS

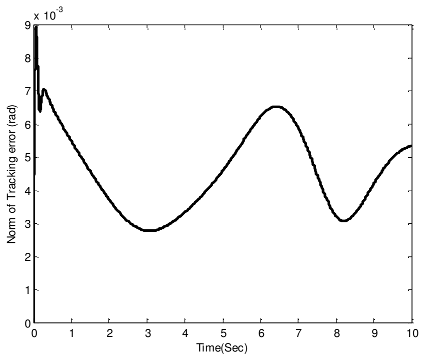

Figure 4. Norm of tracking error in JS

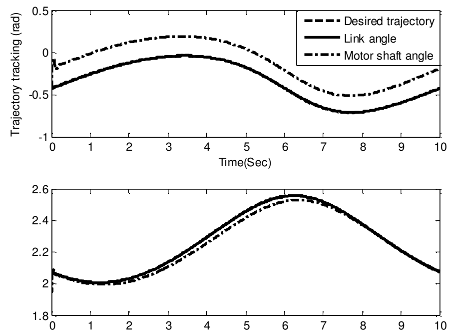

Figure 5. Tracking performance in JS

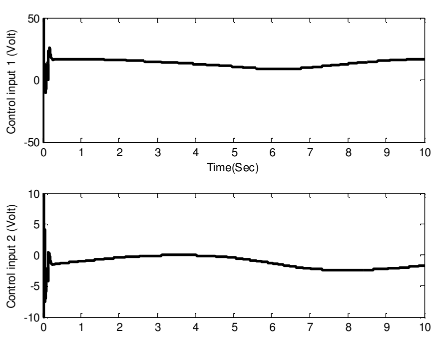

Figure 6. The control efforts for both joints

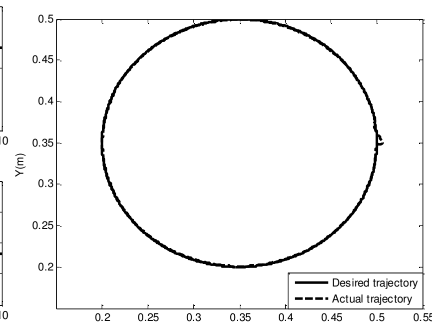

Figure 7. Tracking performance in TS

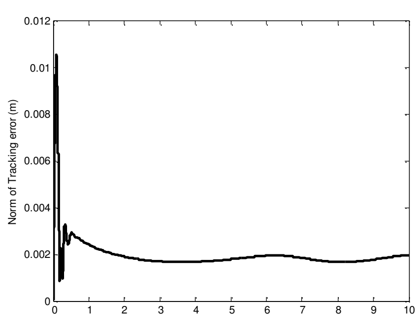

Figure 8. Norm of tracking error in TS

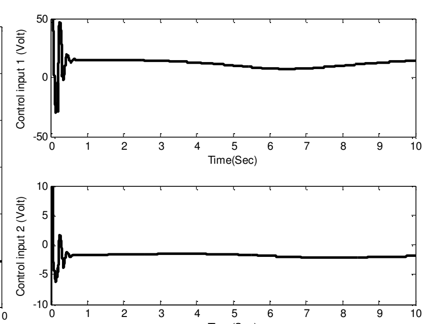

Figure 9. The control efforts for both joints

$R = diag(1.6, 1.6)\Omega$, $k_m = k_b = diag(0.26, 0.26)$(N-m/A), $J_m = diag(2\times10^{-4}, 2\times10^{-4})(kg\text{-}m^2)$, $B_m = diag(10^{-3}, 10^{-3})$(N-m-sec/rad), $L = diag(10^{-3}, 10^{-3})$ (H), $K = diag(500, 500)$(N-m/rad), and $r = diag(0.02, 0.02)$. The manipulator end-effector is commanded to follow a circular trajectory specified by 0.15m radius centered at (0.35m,0.35m), in the TS. The forward kinematic equation is given by

$$X = l_1 cos(q_1) + l_2 cos(q_1 + q_2)$$
$$Y = l_1 sin(q_1) + l_2 sin(q_1 + q_2) \quad (45)$$

The manipulator Jacobian matrix $J(q)$ mapping from TS to JS is bounded and given by

$$J(q) = \begin{bmatrix} -l_1 sin(q_1) - l_2 sin(q_1 + q_2) & -l_2 sin(q_1 + q_2) \\ l_1 cos(q_1) + l_2 cos(q_1 + q_2) & l_2 cos(q_1 + q_2) \end{bmatrix} \quad (46)$$

The link's length is estimated by a gain of 0.6 from real values defined as before. The initial tracking error s are selected zero in all simulations. To clarify the significance of the proposed controller two-simulation set will be investigated.

Simulation 1: The JS controller given by (18)-(22) are simulated to track a circle in TS. For the purpose of simulation, we set $c_1 = 50$, $K_d = 70$, $K_p = 1500$, and $K_i = 2000$. Figure. 2 shows the tracking performance of the robot endpoint and its desired trajectory in the TS. The norm of tracking error in TS indicates a maximum value of 430mm, while the norm of joint errors is negligible with a maximum value of 7×10^{-3} rad as shown in Figure. 3, and Figure. 4 respectively. Therefore, despite of good tracking performance of the robust JS control strategies in JS, shown by Figure. 5, they cannot provide satisfactory performance in TS under imperfect transformation of control space. The efforts to the two joints are reasonable that can be verified in Figure. 6. As a result, the performance of the JS control strategies is degraded by the imperfect transformation.

Simulation 2: The proposed TS control strategy given by (20)-(22) and (41) are simulated where the control parameters are $c_1 = 10$, $K_d = 20$, $K_p = 800$, $K_i = 1500$, and $\varepsilon = 0.4$. Figure. 7 shows the end-effector position of robot manipulator in the x-y-directions under %40 uncertainties and without any knowledge of robotic manipulator dynamic. As can be seen from Figure. 8, end-effector positions converge nicely to the desired value in TS. The profile of actuator voltage is shown in Figure. 9. The simulation results verify the good tracking performance of the proposed controller to robustly stabilize the system, while achieving robust performance subject to uncertainties in kinematic and dynamic equations.

CONCLUSION

Many robust control techniques have been designed to control of robot manipulator in JS under uncertainties. However, control performance is degraded under imperfect transformation of control space from TS to JS. This paper presents a robust TS controller to cope with the tracking problem of flexible joint electrically driven robots. The proposed approach is free from robot manipulator dynamic. It is shown that the robotic system has the Bounded Input-Bounded Output (BIBO) stability in the sense that all the signals are bounded. Numerical results for a two-link flexible joint robot driven by permanent magnet dc motors have shown the superiority of TS controller to the JS controller. The tracking performance is satisfactory such that the flexibility of the robotic system has been well under control. The control efforts are continuous and soft to be easily implemented. The performance of control system verifies that the control system is robust against all uncertainties in manipulator dynamics and its motors. The voltages of motors are permitted under the maximum values.

REFERENCES

Cheah CC, Liu C, Slotine JJE (2010). Adaptive Jacobian Vision Based Control for Robots With Uncertain Depth Information, Automatica. 46:1228-1233,

Chen Ch-Sh (2011). Robust Self-Organizing Neural-Fuzzy Control With Uncertainty Observer for MIMO Nonlinear Systems, IEEE Trans. on Fuzzy Systems. 19(4): 694-706,

Chien M-Ch, Huang AC (2010). A Regressor-free Adaptive Control for Flexible-joint Robots based on Function Approximation Technique, Chapter 2 in the book Advances in Robot Manipulators, I-Tech Education and Publishing, Vienna, Austria,

Colbaugh R, Glass K (1997). Adaptive Task-Space Control of Flexible-Joint Manipulators, Journal of Intelligent and Robotic Systems. 20:225-249,

Faroog M, Wang DB, Dar NU (2008).Hybrid Force/Position Control Scheme for Flexible Joint Robot With Friction Between and the End-Effector and the Environment, Int. J. Eng. Sci. 46:1266-1278

Fateh MM (2008). On the Voltage-Based Control of Robot Manipulators, International Journal of Control, Automation and Systems. 6(5):702-712,

Fateh MM (2012). Nonlinear Control of Electrical Flexible-Joint Robots, Nonlinear Dynamic. 67(4):2549-2559.

Fateh MM (2012). Robust Control of Flexible-Joint Robots Using Voltage Control Strategy, Nonlinear Dynamic, 67(2):1525-1537.

Fateh MM, Farhangfard H (2008). On the Transforming of Control Space by Manipulator Jacobian, International Journal of Control, Automation and Systems. 6(1):101-108,

Ghorbel F, Hung JY, Spong MW (1989). Adaptive Control of Flexible Joint Manipulators, IEEE Control System Magazine. 9 (7): 9-13,

Goldsmith PB, Francis BA, Goldenberg AA (1999). Stability of Hybrid Position/Force Control Applied to Manipulators With Flexible Joints, Int. Jour. Of. Robotics and Automation. 14(4):146-160

Hu Y-R, Vukovich G (2001). Position and Force Control of Flexible Joint Robots During Constrained Motion Tasks, Mechanism and Machine Theory. 36:853-871.

Lee J, Yeon JS, Park JH, Lee S (2007). Robust Back-Stepping Control for Flexible-Joint Robot Manipulators, IEEE/RSJ International Conference on Intelligent Robots and Systems. 183-188,

Liu C, Cheah CC, Slotine JJE (2008). Adaptive Task-Space Regulation of Rigid-Link Flexible-Joint Robots With Uncertain Kinematics, Automatica. 44:1806-1814.
Luca AD, Isidori A, Nicolo F (1985). Control of Robot Arm with Elastic Joints Via Nonlinear Dynamic Feedback, The 24th Conf. Decision and Contr. 1671– 1679,
Morris AS (2001). Measurement and Instrumentation Principles, Butterworth-Heinemann.
Spong MW(1987). Modeling and Control of Elastic Joint Robots. ASME J. Dyn. Syst. Meas. Control, 109:310–319
Spong MW, Khorasani K, Kokotovic PV (1987). An Integral Manifold Approach to the Feedback Control of Flexible Joint Robots. IEEE J. Robot. Autom. 291–300
Spurgeon SK, Yao L, Lu XY (2001). Robust Tracking Via Sliding Mode Control for Elastic Joint Manipulators, Proc. Inst. Mech. Eng. I. 215(4):405-417,
Subudhi B, Morris AS (2006).Singular Perturbation Based Neuro-H∞ Control Scheme for a Manipulator with Flexible Links and Joints, Robotica, 24:151–161.
Talole E, Kolhe P, Phadke B(2010). Extended State Observer Based Control of Flexible Joint System With Experimental Validation. IEEE Trans. Ind. Electron. 57(4):1411-1419,
Tian L, Goldenberg A (1995). Adaptive and Sliding Control of Flexible Joint Robots in Constrained motion, IEEE International Conference on Systems, Man and Cybernetics. 4161 – 4166,
Tian L, Wang J, Mao Z (2004). Constrained Motion Control of Flexible Robot Manipulators based on Recurrent Neural Networks, IEEE Trans. on Syst. Man Cybern. Part B. 34(3):1541-1552,
Tomei P (1991). A Simple PD Controller for Robots with Elastic Joints, IEEE Trans. on. Autom. Control. 36(10):1208–1213
Wang D (1995). A Simple Iterative Learning Controller for Manipulators With Flexible Joints, Automatica. 31(9): 1341–1344,
Zeman V, Patel RV, Khorasani K (1997). Control of a Flexible-J Robot Using Neural Networks, IEEE Trans. Control Syst. Technol. 5(4): 453–462.